

WHITE DWARF HEATING AND SUBSEQUENT COOLING IN DWARF NOVA OUTBURSTS

ANTHONY L. PIRO

Department of Physics, Broida Hall, University of California,
Santa Barbara, CA 93106; piro@physics.ucsb.edu

PHIL ARRAS

NSF AAMPF Fellow, Kavli Institute for Theoretical Physics, Kohn Hall, University of California,
Santa Barbara, CA 93106; arras@kitp.ucsb.edu

AND

LARS BILDSTEN

Kavli Institute for Theoretical Physics and Department of Physics, Kohn Hall, University of California,
Santa Barbara, CA 93106; bildsten@kitp.ucsb.edu

Accepted for publication in The Astrophysical Journal

ABSTRACT

We follow the time dependent thermal evolution of a white dwarf (WD) undergoing sudden accretion in a dwarf nova outburst, using both simulations and analytic estimates. The post-outburst lightcurve clearly separates into early times when the WD flux is high, and late times when the flux is near the quiescent level. The break between these two regimes, occurring at a time of order the outburst duration, corresponds to a thermal diffusion wave reaching the base of the freshly accreted layer. Our principal result is that long after the outburst, the fractional flux perturbation about the quiescent flux decays as a power law with time (and *not* as an exponential). We use this result to construct a simple fitting formula that yields estimates for both the quiescent flux and the accreted column, i.e. the total accreted mass divided by WD surface area. The WD mass is not well constrained by the late time lightcurve alone, but it can be inferred if the accreted mass is known from observations. We compare our work with the well-studied outburst of WZ Sge, finding that the cooling is well described by our model, giving an effective temperature $T_{\text{eff}} = 14,500$ K and accreted column $\Delta y \approx 10^6$ g cm⁻², in agreement with the modeling of Godon et al. To reconcile this accreted column with the accreted mass inferred from the bolometric accretion luminosity, a large WD mass $\gtrsim 1.1M_{\odot}$ is needed. Our power law result is a valuable tool for making quick estimates of the outburst properties. We show that fitting the late time lightcurve with this formula yields a predicted column within 20% of that estimated from our full numerical calculations.

Subject headings: accretion, accretion disks — novae, cataclysmic variables — stars: individual (WZ Sagittae) — white dwarfs

1. INTRODUCTION

Dwarf novae (DNe) are cataclysmic variables (CVs; Warner 1995) that undergo dramatic accretion events in which a large fraction of the accretion disk is dumped onto the white dwarf (WD) surface. These last for $\sim 2-20$ days at accretion rates of $\sim 10^{-8}M_{\odot}$ yr⁻¹ and are separated by quiescent intervals of ~ 10 days to tens of years. Following DN outbursts, CVs show a decreasing ultraviolet flux (e.g., Long et al. 1994; Gänsicke & Beuermann 1996; Sion et al. 1996; Szkody et al. 1998; Cheng et al. 2000). The accretion rate then is low enough that the WD surface can be directly seen, and spectroscopic observations indicate this flux originates from a WD cooling in response to the outburst (Mateo & Szkody 1984; Kiplinger, Sion, & Szkody 1991; Long et al. 1993; Sion 1993). The flux converges asymptotically to a quiescent level set by the time-averaged accretion rate (Townsend & Bildsten 2003), $F_0 = \sigma_{\text{SB}} T_{\text{eff},0}^4$, where σ_{SB} is the Stefan-Boltzmann constant and $T_{\text{eff},0}$ is the quiescent WD effective temperature.

The lightcurve of the cooling WD depends on the mechanism for heating, which has previously been attributed to boundary layer irradiation (Regev 1983; Pringle 1988; Regev & Shara 1989; Godon, Regev, & Shaviv 1995; Popham 1997), compressional heating (Sion 1995; Godon & Sion 2002), and shear mixing luminos-

ity (Sparks et al. 1993). For a covering fraction $\lesssim 0.1$ (Piro & Bildsten 2004), we show in the Appendix that boundary layer heating (even via shear mixing) and surface advection have a negligible impact on the late time cooling lightcurve as long as the imposed surface temperatures are $\lesssim 10^6$ K. Temperatures higher than this are ruled out according to theoretical work on the boundary layer (Popham & Narayan 1995; Piro & Bildsten 2004). We therefore focus solely on compressional heating to understand the cooling flux released on long timescales. We show that this late time cooling is a powerful tool for studying DN outbursts as it is independent of the time dependent accretion rate during the outburst. Furthermore, WD photospheric temperature estimates are less uncertain well after the outburst since any residual screening material has dissipated (see Long et al. 2004).

We present numerical calculations following the compressional heating and subsequent cooling of the WD surface in §2. We investigate the late time cooling analytically in §3, showing that it obeys a power law, and not an exponential decay (as has been assumed in other studies, for example in Gänsicke & Beuermann 1996). Furthermore, this power law is not in temperature, but rather in the *fractional temperature perturbation about the quiescent WD temperature*, $\delta T_{\text{eff}}/T_{\text{eff},0}$. We construct a fitting formula (eq. [20]) that can be applied to

DN cooling observations to constrain both the quiescent flux, $F_0 = \sigma_{SB} T_{\text{eff},0}^4$, and the column of material accreted during the DN outburst, $\Delta y = \Delta M / (4\pi R^2)$ (using eq. [22]), where ΔM is the total amount of mass accreted. This late time lightcurve depends weakly on the surface WD gravity, and therefore cannot directly constrain the WD mass. However, if ΔM is known from other observations, the WD radius (and mass) can be inferred. We compare our model to the 2001 July outburst of WZ Sge in §4, and show that its cooling is consistent with our model. Our analytic formula fits the late time lightcurve and yields an accreted column to within 20% of that found from our full numerical calculation. We conclude in §5 by summarizing our results and discussing the importance of further, multi-epoch observations of WD cooling following DN outbursts. An appendix investigates the impact of surface heating on the late time cooling lightcurve.

2. TIME EVOLUTION DURING THE DWARF NOVA OUTBURST

In this section we present time dependent numerical models of WD thermal evolution during and after a DN outburst. These highlight the importance of deep compressional heating, which will be useful for constructing the analytic late time cooling curves.

2.1. Quiescent White Dwarf Model

We begin by describing the quiescent background model of the WD envelope, as expected between outbursts when the accretion rate is low ($\dot{M} \lesssim 10^{-11} M_\odot \text{ yr}^{-1}$). We focus on shallow, radiative surface layers of the WD, which we model with plane parallel geometry and constant gravitational acceleration, $g = GM/R^2$. It is convenient to use column depth $y = -\int \rho dr$ as a vertical coordinate, where r is the spherical radius. Hydrostatic balance then becomes $P = gy$. Throughout this paper we give numerical estimates using solar composition, ideal, nondegenerate gas and Kramer's opacity. We made comparisons with a more detailed calculation using OPAL opacities (Iglesias & Rogers 1996) and did not find significant deviations from our results. For solar composition and gravity $g = 10^8 \text{ cm s}^{-2}$, surface convection zones are confined to columns $y \lesssim 1 \text{ g cm}^{-2}$ for $T_{\text{eff}} \gtrsim 11,000 \text{ K}$, and can be ignored.

In quiescence, the thermal profile is set by the underlying flux from the core, determined by the time-averaged accretion rate (Townsend & Bildsten 2003). The WD surface layers are described by the radiative flux equation

$$F = \frac{16\sigma_{SB} T^3}{3\kappa} \frac{\partial T}{\partial y}, \quad (1)$$

where F is the outward directed flux, σ_{SB} is the Stefan-Boltzmann constant and κ is the opacity, which we assume satisfies a power law $\kappa = \kappa_0 \rho^a T^b$. For Kramer's opacity $a = 1$, $b = -7/2$, and $\kappa_0 = 6.5 \times 10^{22}$ (in cgs units). Denoting the quiescent flux by $F_0 = \sigma_{SB} T_{\text{eff},0}^4$, we integrate equation (1) to find the temperature profile in quiescence

$$T_0(y) = \left[(n+1) \frac{F_0}{\alpha} \right]^{1/(4+a-b)} y^{1/(n+1)} \\ = 5.7 \times 10^5 \text{ K } g_8^{2/17} F_{0,12}^{2/17} y_5^{4/17}, \quad (2)$$

where $g_8 \equiv g/10^8 \text{ cm s}^{-2}$, $F_{0,12} \equiv F_0/10^{12} \text{ erg s}^{-1} \text{ cm}^{-2}$, $y_5 \equiv y/10^5 \text{ g cm}^{-2}$, $n = (3-b)/(1+a)$ is the polytrope index ($n = 13/4$ for Kramer's opacity), and $\alpha \equiv (16\sigma_{SB}/3\kappa_0)(k_b/\mu m_p g)^a = 6.2 \times 10^{-27} g_8^{-1}$ (in cgs units).

A property of the envelope that is important for understanding the cooling is the local thermal time at a column depth y ,

$$t_{\text{th},0}(y) = \frac{y c_p T_0(y)}{F_0} \\ = \frac{c_p}{F_0} \left[(n+1) \frac{F_0}{c_p} \right]^{1/(4+a-b)} y^{(n+2)/(n+1)} \\ = 0.73 \text{ yr } g_8^{2/17} F_{0,12}^{-15/17} y_5^{21/17}, \quad (3)$$

where $c_p \approx 5k_B/(2\mu m_p)$ is the specific heat, k_B is Boltzmann's constant, and $\mu = 0.62$ is the mean molecular weight in the nondegenerate plasma of solar composition.

2.2. Compressional Heating During the Outburst

The entropy equation describing time evolution of the WD temperature profile during the DN outburst can be written as (Bildsten 1998)

$$\frac{\partial F}{\partial y} = c_p \left[\frac{\partial T}{\partial t} + \frac{\dot{m} T}{y} (\nabla - \nabla_{\text{ad}}) \right], \quad (4)$$

where $\dot{m} \equiv \dot{M}/(4\pi R^2)$ is the accretion rate per unit area, $\nabla \equiv \partial \ln T / \partial \ln y$ is found from equation (1), and $\nabla_{\text{ad}} \equiv (\partial \ln T / \partial \ln P)_{\text{ad}} \approx 2/5$ sets the adiabatic profile. The second term on the right hand side arises from the advection of entropy $v_r \partial s / \partial r = (-\dot{m}/\rho) \partial s / \partial r = \dot{m} \partial s / \partial y$ by the accretion flow, where v_r is the advection velocity and s is the specific entropy.

We solve equations (1) and (4) implicitly in time using backward time differencing for stability and typically 128 to 512 grid points. The time step is chosen so that the average temperature at each grid point changes by a fractional amount $\lesssim 10^{-3}$ from one time step to the next. We repeated a number of runs with a fractional change of 10^{-4} and the results did not change. The boundary condition at the base of the layer is taken to be constant flux, F_0 , and set at a depth ($\approx 10^8 \text{ g cm}^{-2}$) where the local thermal time is longer than any timescale of interest (i.e. longer than the time we wish to follow the cooling). The flux into the core does change due to each DN outburst, but by a tiny amount of order the ratio of the mass accreted in one DN outburst to the envelope mass. As we do not model the photosphere, the surface boundary condition is set at a shallow depth with a sufficiently short thermal time for the temperature profile to be constant flux, $T \propto y^{1/(n+1)}$. The initial condition for the outburst is the constant flux profile in equation (2). This is evolved forward for a time t_{dno} , with mass accretion set by a given function $\dot{m}(t)$.

In Figure 1 we plot the heating profiles during a DN outburst at 10 different times, spaced logarithmically from 0.52 to 52 days. The WD has $T_{\text{eff},0} = 14,500 \text{ K}$ and $g = 10^8 \text{ cm s}^{-2}$ (as appropriate for an $M = 0.6 M_\odot$ WD), and accretes at a constant rate $\dot{m} = 0.30 \text{ g cm}^{-2} \text{ s}^{-1}$ [a global accretion rate of $6 \times 10^{-8} M_\odot \text{ yr}^{-1} (R/10^9 \text{ cm})^2$], giving a total accreted column $\Delta y = 1.3 \times 10^6 \text{ g cm}^{-2}$. We focus on the fractional temperature and flux profiles, $\delta T(y,t)/T_0(y) = (T(y,t) - T_0(y))/T_0(y)$ and $\delta F(y,t)/F_0 = (F(y,t) - F_0)/F_0$, respectively, as we later show that these quantities obey power laws at late times.

The bottom panel in Figure 1 shows the flux perturbation as a function of depth, increasing in time from bottom to top. Two distinct regimes are seen for $\delta F/F_0$, separated by the base of the accreted layer, shown by dots. Above this depth, the profiles are determined by the steady state solutions to equation (4), while below the perturbations are small and

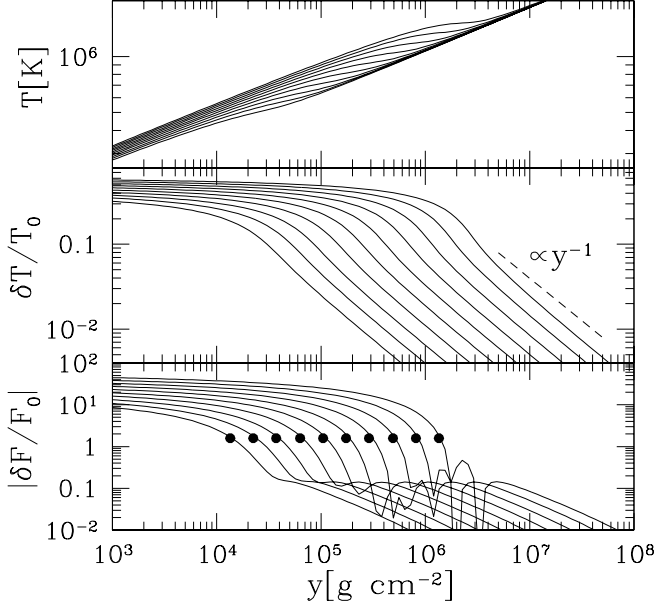


FIG. 1.— Temperature, T , fractional temperature perturbation, $\delta T/T_0$, and fractional flux perturbation, $|\delta F/F_0|$, during accretion with $\dot{m} = 0.30 \text{ g cm}^{-2} \text{ s}^{-1}$, $t_{\text{dno}} = 52$ days, and $T_{\text{eff},0} = 14,500 \text{ K}$. The 10 curves are logarithmically spaced in time from 0.52 to 52 days, from bottom to top. The dots in the bottom panel mark the base of the accreted layer, $\dot{m}t$. At some depths $F(y,t) < F_0$, so that $\delta F/F_0 < 0$. Since we plot the quantities logarithmically to emphasize the power laws, we must take the absolute value of $\delta F/F_0$, which creates the jumps seen in the bottom panel whenever $\delta F/F_0$ passes through zero.

largely due to adiabatic compression. The middle panel shows the fractional temperature perturbation. Near the surface, this quantity is fairly constant with a slight decrease with depth, but below the base of the accreted layer it falls off as a power law $\delta T/T_0 \propto y^{-1}$ for adiabatic compression. Finally, the absolute temperature is shown in the top panel. The flattening of the temperature profile near the base of the accreted layer is apparent, especially at late times. If the outburst had lasted longer, or the accretion rate was higher, a temperature inversion would have developed just below the base of the accreted layer. Since t_{th} is short in these shallow layers, such an inversion “smooths out” very quickly once the envelope begins to cool and has a negligible effect on the cooling lightcurve.

The final profile after the DN event can be understood by comparing the timescales of equation (4), which are the accretion time $t_{\text{acc}} = y/\dot{m}$, the thermal time $t_{\text{th}} = y c_p T/F$, and the elapsed time t . Above the base of the accreted layer, $y \ll \dot{m}t$, there is a hierarchy of timescales $t_{\text{th}} \ll t_{\text{acc}} \ll t$, so that we take $\partial/\partial t \approx 0$. The flux near the surface is nearly constant, with a small decrease with depth due to compressional heating. Denoting the (constant) surface flux as F_s , we find the temperature profile associated with this, which we denote $T_s(y)$, by using equation (2) with F_0 replaced by F_s . Substituting $T_s(y)$ into equation (4) and integrating we find

$$F(y) \approx F_s - \left(\frac{\nabla_{\text{ad}}}{\nabla} - 1 \right) \dot{m} c_p T_s(y). \quad (5)$$

This shows how the flux decreases near the surface, as can be seen in Figure 1. The true temperature profile is therefore smaller than the constant flux profile, $T_s(y)$, and can be estimated by substituting equation (5) into equation (1) and

integrating,

$$T(y) \approx T_s(y) \left[1 - \frac{1}{5+a-b} \left(\frac{\nabla_{\text{ad}}}{\nabla} - 1 \right) \frac{\dot{m} c_p T_s(y)}{F_s} \right]. \quad (6)$$

Setting $F \sim 0$ at the base of the accreted layer, $y \approx \dot{m}t_{\text{dno}}$ (see Figure 1), we can estimate the flux F_s as a function of t_{dno} . This implies an effective temperature during accretion

$$\begin{aligned} T_{\text{eff}} &= \left(\frac{F_s}{\sigma_{\text{SB}}} \right)^{1/4} \\ &\approx 3.0 \times 10^4 \text{ K } g_8^{1/30} \\ &\times \left(\frac{\dot{m}}{0.3 \text{ g cm}^{-2} \text{ s}^{-1}} \right)^{7/20} \left(\frac{t_{\text{dno}}}{1 \text{ day}} \right)^{1/15}, \quad (7) \end{aligned}$$

which agrees with our numerical models. This power law index of $1/15 \approx 0.067$ is similar to the power laws found by Godon & Sion (2003) during heating. We also agree that the power law during heating is for the actual effective temperature (as opposed to the *fractional* effective temperature as we find for the cooling). Since this evolution takes place coincident with a high accretion rate, it will not be observable so we do not elaborate on its effects any more here.

We now derive the profile for $\delta T/T_0$ deep in the envelope due to adiabatic compression. This is the first step in understanding late time cooling. Well below the base of the accreted layer, $y \gg \Delta y$, the timescales satisfy $t \ll t_{\text{acc}} \ll t_{\text{th}}$. The initial temperature profile from equation (2) is compressed adiabatically, giving

$$\begin{aligned} T(y) &= T_0(y - \Delta y) \left(\frac{y}{y - \Delta y} \right)^{\nabla_{\text{ad}}} \\ &\approx T_0(y) \left[1 + (\nabla_{\text{ad}} - \nabla) \frac{\Delta y}{y} \right], \quad (8) \end{aligned}$$

or, a fractional temperature perturbation

$$\frac{\delta T}{T_0} \approx (\nabla_{\text{ad}} - \nabla) \frac{\Delta y}{y}, \quad (9)$$

which explains the scaling $\delta T/T_0 \propto y^{-1}$ in Figure 1. This extends from deep in the envelope up to $y \approx \Delta y = \dot{m}t_{\text{dno}}$.

2.3. Cooling Following the Outburst

We evolve the final profile from Figure 1 forward in time to see how the WD cools after accretion has halted. Again we solve equations (1) and (4), but now with $\dot{m} = 0$. In Figure 2 we show profiles during cooling spaced logarithmically in time from 10 to 1000 days after the end of the outburst. Near the surface, the profiles show constant perturbations $\delta F/F_0$ and $\delta T/T_0$, while at large depths the profile is unevolved. Just as during heating, $\delta F/F_0$ is an order of magnitude larger than $\delta T/T_0$, which we explain in §3 when we derive self-similar solutions for the cooling phase.

From this example we see that cooling involves a thermal wave moving into the envelope, propagating down to a column y only at a time, $t \approx t_{\text{th}}(y)$. This is simplest to show for the deep, adiabatically compressed material. Since the perturbations at these depths are small, we approximate $t_{\text{th}} \approx t_{\text{th},0}$. Setting $t_{\text{th},0} = t$ we invert equation (3) to find the column that is just beginning to cool as a function of time,

$$\begin{aligned} y_{\text{th}}(t) &= \left(\frac{F_0}{c_p} \right)^{(n+1)/(n+2)} \left[\frac{\alpha}{(n+1)F_0} \right]^{1/(n+2)} t^{(n+1)/(n+2)} \\ &\approx 1.3 \times 10^5 \text{ g cm}^{-2} g_8^{-2/21} F_{0,12}^{15/21} \left(\frac{t}{1 \text{ yr}} \right)^{17/21}, \quad (10) \end{aligned}$$

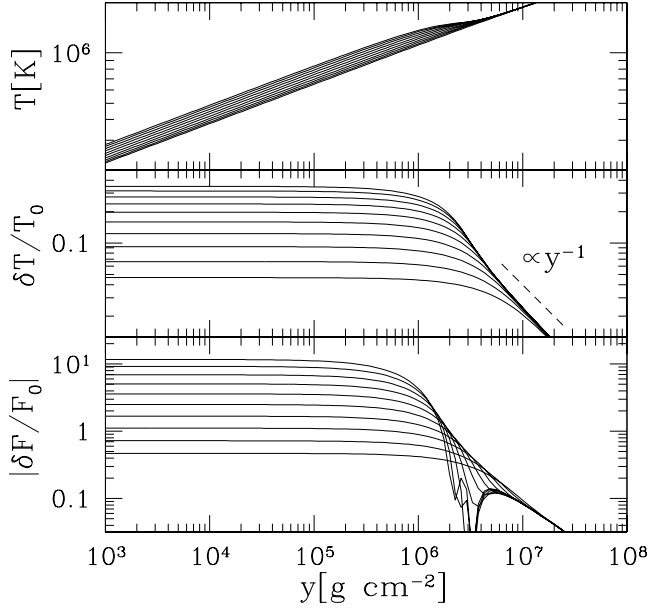


FIG. 2.— Profiles for T , $\delta T/T_0$, and $|\delta F/F_0|$ during the cooling following the outburst presented in Figure 1, in which a column $\Delta y = 1.3 \times 10^6 \text{ g cm}^{-2}$ was accreted in $t_{\text{th}0} = 52$ days. The 10 curves are logarithmically spaced in time from 10 to 1000 days, from top to bottom.

where t is measured from the end of the outburst. Substituting this result for y in equation (9), we find that the late time cooling should evolve according to $\delta T/T_0 \sim (\nabla_{\text{ad}} - \nabla) \Delta y / y_{\text{th}}(t) \propto t^{-(n+1)/(n+2)}$. As we shall see in §3, this estimate is correct up to a numerical factor that can be computed.

In the Appendix we consider the effects of boundary layer heating on this late time cooling. We find that surface heating only propagates a finite distance into the envelope, while compressional heating causes a $\delta T/T_0 \propto y^{-1}$ perturbation down to arbitrarily large depths, so that at very late times compressional heating always dominates. In practice, this may occur so long after the outburst that during the observational period both heating mechanisms must be considered for proper modeling. This happens when the boundary layer is too hot, so that a diffusion wave propagating from the surface does not have sufficient time to reach the background quiescent profile during heating, resulting in a critical boundary layer temperature (eq. [A4]),

$$T_{\text{bl,crit}} \sim 10^6 \text{ K } g_8^{2/17} F_{0,12}^{2/17} \left(\frac{\Delta y}{10^6 \text{ g cm}^{-2}} \right)^{4/17}. \quad (11)$$

This critical temperature is close to, but most likely ruled out by observations (Mauche 2004) and theoretical modeling (Popham & Narayan 1995; Piro & Bildsten 2004).

3. SELF-SIMILAR COOLING

In §2.3, we found that the fractional temperature perturbation decreases as a simple power law with time for late time cooling after an outburst. We now provide a rigorous derivation of the power law index and calculate the prefactor.

The discussion in §2.3 suggests that the late time cooling is governed by the self-similarity variable

$$\xi(y, t) = \left[\frac{t_{\text{th},0}(y)}{t} \right]^{1/2} = \left[\frac{y}{y_{\text{th}}(t)} \right]^{(n+2)/(2(n+1))}, \quad (12)$$

where t is measured from the end of the outburst, and we have introduced the $1/2$ -power for calculational convenience. At large depths, the initial temperature profile is given by equation (9), so we make the ansatz

$$\delta T(y, t) = T_0(y) (\nabla_{\text{ad}} - \nabla) \frac{\Delta y}{y} f(\xi), \quad (13)$$

where $f(\xi)$ is an undetermined function that contains the time dependence of the temperature perturbation. To understand the late time cooling we now find f for large t (i.e. in the limit $\xi \rightarrow 0$).

Taking perturbations of equation (4) about the quiescent profile (with $\dot{m} = 0$) gives

$$c_p \frac{\partial \delta T}{\partial t} = \frac{\partial \delta F}{\partial y}, \quad (14)$$

where the perturbed flux is

$$\frac{\delta F}{F_0} = (n+1) \frac{\partial}{\partial \ln y} \left(\frac{\delta T}{T_0} \right) + (4+a-b) \frac{\delta T}{T_0}. \quad (15)$$

We substitute the perturbed temperature from equation (13) into equations (14) and (15), which are then combined to give a single equation for f ,

$$\xi \frac{df}{d\xi} \left[\frac{\xi^2}{2} - (n+2) + \frac{(n+2)^2}{4(n+1)} + \frac{(n+2)}{2(n+1)} (4+a-b) \right] + \frac{(n+2)^2}{4(n+1)} \xi^2 \frac{d^2 f}{d\xi^2} + f [n+1 - (4+a-b)] = 0. \quad (16)$$

In the limit $\xi \rightarrow \infty$, $f \rightarrow 1$ by definition. In the other limit of $\xi \rightarrow 0$, equation (16) has a finite solution $f = \eta \xi^{2(n+1)/(n+2)}$, where η is a constant of proportionality determined by the full numerical solution. Since equation (16) contains unwanted solutions that are strongly divergent, we solve it as a matrix equation, finding $\eta = 0.141$ for Kramer's opacity. The late time temperature perturbation is then

$$\frac{\delta T(y, t)}{T_0(y)} = \eta (\nabla_{\text{ad}} - \nabla) \frac{\Delta y}{y_{\text{th}}(t)}, \quad (17)$$

which is what we guessed in §2.3, up to the factor η .

To make comparisons with the observed late time cooling, we relate the above analysis to the fractional T_{eff} perturbation, $\delta T_{\text{eff}}/T_{\text{eff},0} = (T_{\text{eff}} - T_{\text{eff},0})/T_{\text{eff},0} \approx \delta F/4F_0$. At late times,

$$\frac{\delta T}{T_0} \propto y^{-1} \xi^{2(n+1)/(n+2)} \approx \text{constant in } y. \quad (18)$$

Equation (15) then relates the temperature and flux perturbations

$$\frac{\delta F}{F_0} \approx (4+a-b) \frac{\delta T}{T_0}, \quad (19)$$

where the factor $4+a-b = 8.5$ explains the order of magnitude difference between $\delta F/F_0$ and $\delta T/T_0$. Both $\delta F/F_0$ and $\delta T/T_0$ are constant in space in the limit $t \gg t_{\text{th}}(y)$. We put these results together to express the change of δT_{eff} in the linear limit in the form

$$\frac{\delta T_{\text{eff}}}{T_{\text{eff},0}} \approx \left(\frac{t_{\text{late}}}{t} \right)^{(n+1)/(n+2)}, \quad (20)$$

where t is the time since the outburst ended, the power law index is $(n+1)/(n+2) = 17/21 \approx 0.81$, and the characteristic late time cooling timescale is

$$t_{\text{late}} = \left[\eta \frac{4+a-b}{4} (\nabla_{\text{ad}} - \nabla) \right]^{(n+2)/(n+1)} t_{\text{th},0}(\Delta y) \approx 0.024 t_{\text{th},0}(\Delta y). \quad (21)$$

Observations that fit t_{late} then constrain

$$\Delta y = 1.8 \times 10^4 \text{ g cm}^{-2} \times g_8^{-2/21} \left(\frac{t_{\text{late}}}{1 \text{ day}} \right)^{17/21} \left(\frac{T_{\text{eff},0}}{10^4 \text{ K}} \right)^{60/21}, \quad (22)$$

the total accreted column during the outburst.

Equations (20) and (22) are our central results. We make the following remarks on their use for understanding observations:

- Observations should be plotted as $\delta T_{\text{eff}}/T_{\text{eff},0}$ in order to test whether a power-law is observed. Equation (20) has three parameters, $T_{\text{eff},0}$, t_{late} , and n , the polytrope index. If the wrong $T_{\text{eff},0}$ is used, the late time cooling does not look like a power law with index ≈ 0.81 , giving a useful constraint on $T_{\text{eff},0}$. Figure 3 shows the result for $(T_{\text{eff}}(t) - xT_{\text{eff},0})/xT_{\text{eff},0}$ from the full cooling code, where $x = 0.9, 1.0, 1.1$. At late times, the analytic formula given by equations (20) and (22) agrees well. When the wrong quiescent effective temperature is used the lightcurve either does not look like a power law (as in the case of too large of a $T_{\text{eff},0}$, i.e. $x = 1.1$), or shows a power law that differs considerably from a power law index of 0.81 (as in the case of too small of a $T_{\text{eff},0}$, i.e. $x = 0.9$).
- If the temperature perturbation $\delta T_{\text{eff}}/T_{\text{eff},0} \gtrsim 0.1$, effects second order in $\delta T_{\text{eff}}/T_{\text{eff},0}$ cause the lightcurve to deviate slightly from a power law, as is apparent in Figure 3 for $x = 1.0$ and $t \lesssim 400$ days. However, adjusting $T_{\text{eff},0}$ until the data is nearly a power law with index 0.81 and applying the analytic formula gives quick results accurate to $\sim 20\%$. We discuss this point in more detail in §4.
- Given a measurement of t_{late} , we can constrain $\Delta y g^{2/21}$ using equation (22). If we allow WDs in the mass range $0.6 - 1.2 M_{\odot}$, the factor $g^{2/21}$ can vary by $\sim 6^{2/21} \approx 1.2$. Therefore, if the WD mass is not known, we can constrain Δy , the accreted column to 20%!

If multiple outbursts are observed from the same system, the lightcurves can be compared to infer the relative amount of mass accreted. We combine equations (20) and (22) to find

$$\frac{\Delta M_1}{\Delta M_2} \approx \frac{\delta T_{\text{eff},1}(t)}{\delta T_{\text{eff},2}(t)}, \quad (23)$$

where ΔM is the amount of mass accreted in an outburst and the subscripts refer to the two outbursts. In this way disk instability models can be tested, including understanding the differences between normal DN outbursts and super-outbursts. In Figure 4 we show how this could be done by comparing the lightcurves of two outbursts, one accreting at a rate of $0.30 \text{ g cm}^{-2} \text{ s}^{-1}$ for $t_{\text{dno}} = 52$ days and the other at a rate of $0.15 \text{ g cm}^{-2} \text{ s}^{-1}$ for $t_{\text{dno}} = 26$ days, but both with $T_{\text{eff},0} = 14,500 \text{ K}$, so that four times the mass is accreted in one outburst in comparison with the other. In the top panel we compare the two resulting lightcurves, and in the bottom panel we look at the ratio of these two lightcurves, which shows how this ratio asymptotes to the accreted mass ratio at late times. For this to work correctly, the two lightcurves must be correctly positioned in time, with $t = 0$ corresponding to the end of the outburst. Fortunately, at late times (when this works best) it should not be difficult to do this with enough accuracy (within ~ 10 days) for useful results.

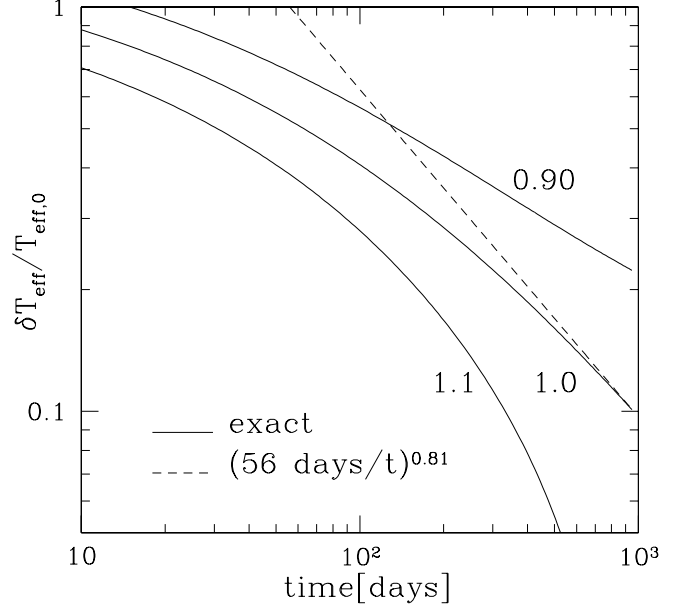


FIG. 3.— The T_{eff} perturbation during cooling from the profiles shown in Figure 2. The three solid lines labeled $x = 0.9, 1.0, 1.1$ represent $(T_{\text{eff}}(t) - xT_{\text{eff},0})/(xT_{\text{eff},0})$, to show how a power law with index ≈ 0.81 only results if the correct $T_{\text{eff},0}$ is used. The analytic formula given in equation (20) is shown by the dashed line.

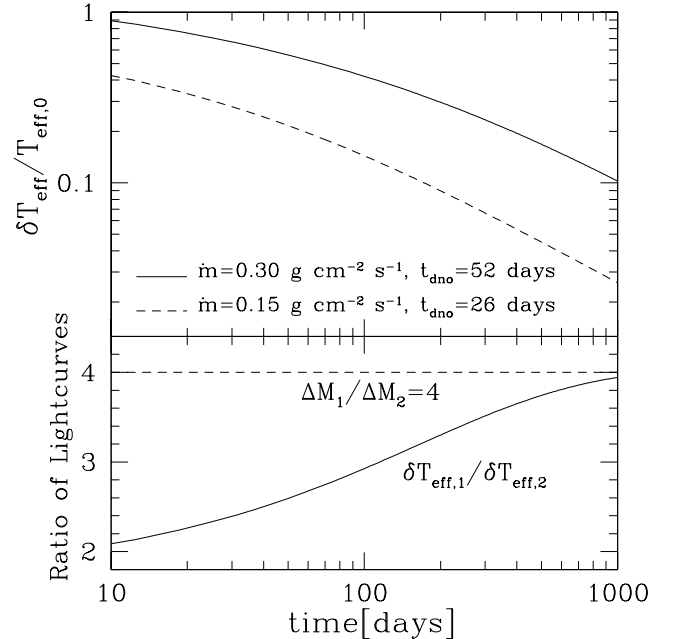


FIG. 4.— A comparison of two outbursts, one accreting at a rate of $0.30 \text{ g cm}^{-2} \text{ s}^{-1}$ for $t_{\text{dno}} = 52$ days and the other at a rate of $0.15 \text{ g cm}^{-2} \text{ s}^{-1}$ for $t_{\text{dno}} = 26$ days, but both with $T_{\text{eff},0} = 14,500 \text{ K}$. This results in four times the mass being accreted in the former outburst in comparison with the latter. In the top panel we show the two resulting $\delta T_{\text{eff}}/T_{\text{eff},0}$ lightcurves, while in the bottom panel we plot the ratio of these two lightcurves. This shows that at late times the ratio asymptotes toward a value equal to the ratio of total accreted masses. A similar study would be useful when considering the multiple outbursts from a given CV.

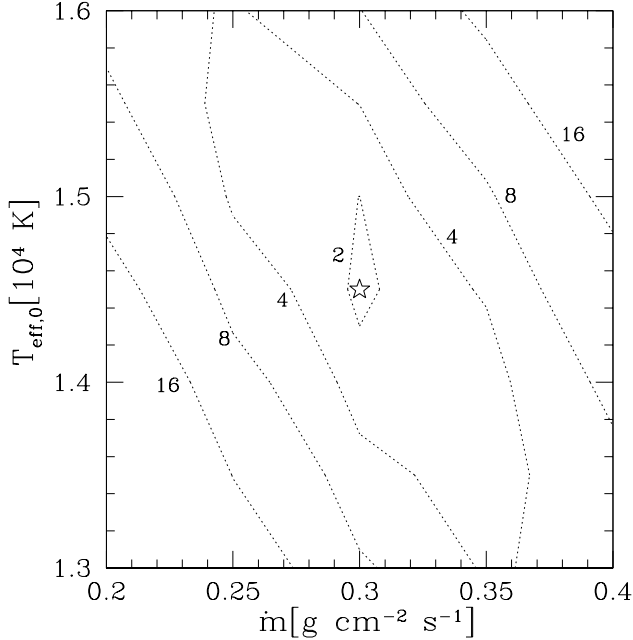


FIG. 5.— Contours of constant χ^2 (dashed lines) from fitting the eight temperature measurements during the cooling of the 2001 July outburst of WZ Sge. We vary both \dot{m} and $T_{\text{eff},0}$ over a grid of our numerical models, but keep $t_{\text{dno}} = 52$ days fixed. The star marks our best fit model, $\dot{m} = 0.30 \text{ g cm}^{-2} \text{ s}^{-1}$ with $T_{\text{eff},0} = 14,500 \text{ K}$.

4. THE 2001 JULY OUTBURST OF WZ SGE

The most detailed observation of a decay after a DN outburst is from the 2001 July 23 outburst of WZ Sge (Ishioaka et al. 2001), providing an excellent test of our cooling model. The outburst lightcurve is complicated (Patterson et al. 2002), initially exhibiting a period of high \dot{M} for 24 days (with a steady decline), a sharp drop in \dot{M} for 3 days, and finally quasi-periodic accretion from days 29 to 52.

The surface temperature of the WD during cooling has been estimated three different ways (Long et al. 2004; Godon et al. 2004). For the sake of comparison, we fit the median temperature measurement (denoted “ T_b ” in Godon et al. 2004), and assume an error $\approx 1000 \text{ K}$ (Gänsicke 2004, private communication). To constrain \dot{m} and $T_{\text{eff},0}$ we calculate χ^2 using the eight temperature measurements of the cooling over a grid of our numerical models, spaced in intervals of $0.05 \text{ g cm}^{-2} \text{ s}^{-1}$ in \dot{m} and 500 K in $T_{\text{eff},0}$. All models assume $t_{\text{dno}} = 52$ days with the accretion rate constant during this time. In Figure 5 we show contours of constant χ^2 , which favors $\dot{m} = 0.30 \text{ g cm}^{-2} \text{ s}^{-1}$ and $T_{\text{eff},0} = 14,500 \text{ K}$ (shown by a star).

In Figure 6 we plot the numerical lightcurve of this favored model along with the corresponding analytic fit using $t_{\text{late}} = 56$ days. At late times the measurement errors are of order the temperature perturbations, which at face value should make comparisons to our numerical models difficult. Fortunately, the data show a clear trend that closely follows the general features of our numerical lightcurve, which strongly suggests that the cooling is due to compressional heating. It has a shallow slope at early times and then becomes a power law at late times with $\delta T_{\text{eff}}/T_{\text{eff},0} \propto t^{-0.81}$ as we predict. Our fit implies an accreted column $\Delta y = 1.3 \times 10^6 \text{ g cm}^{-2} g_8^{-2/21}$, corresponding to an average accretion rate during the outburst

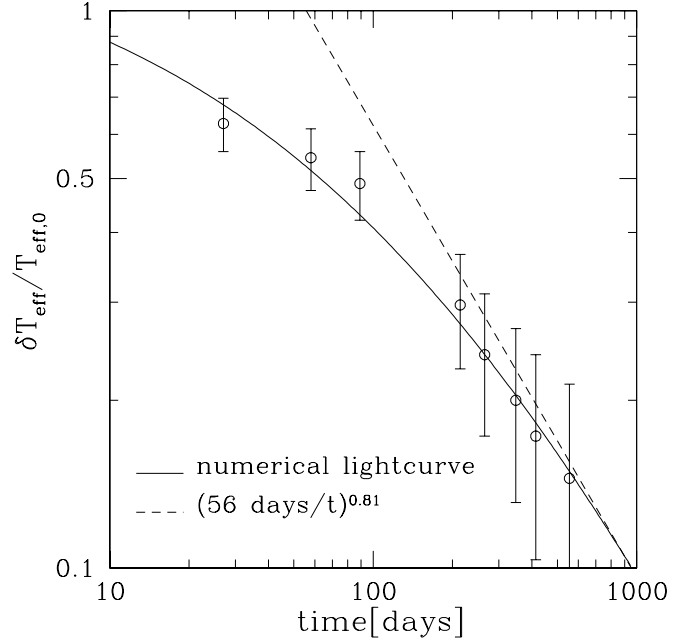


FIG. 6.— The fractional temperature during the 2001 July outburst of WZ Sge in comparison the cooling of a compressional heated envelope. The circles show temperature “ T_b ” from Godon et al. (2004), with the error bars of 1000 K . The solid curve is our numerical calculation with $T_{\text{eff},0} = 14,500 \text{ K}$ and constant $\dot{m} = 0.30 \text{ g cm}^{-2} \text{ s}^{-1}$ for 52 days, giving $\Delta y = 1.3 \times 10^6 \text{ cm}^{-2}$. This corresponds to an average accretion rate of $\langle \dot{M} \rangle \approx 10^{-8} M_{\odot} \text{ yr}^{-1}$ for an $M = 1.1 M_{\odot}$, $R = 5 \times 10^8 \text{ cm}$ WD. The analytic formula given in equation (20) for $t_{\text{late}} = 56$ days is shown by the dashed line.

$\langle \dot{M} \rangle \approx 10^{-8} M_{\odot} \text{ yr}^{-1}$ (assuming a WD radius of $5 \times 10^8 \text{ cm}$, or mass $M = 1.1 M_{\odot}$), in reasonable agreement with the \dot{M} ’s estimated by Long et al. (2003) of $(1-3) \times 10^{-9} M_{\odot} \text{ yr}^{-1}$ (measured when the outburst was especially bright). We therefore favor a massive WD (small radius) to get an \dot{M} closer to these measurements. Such a mass estimate is consistent with the value estimated by Patterson et al. (2002) of $1.0 \pm 0.2 M_{\odot}$. Godon et al. (2004) also find $T_{\text{eff},0} = 14,500 \text{ K}$ and $\Delta y \approx 1.3 \times 10^6 \text{ g cm}^{-2}$ (estimated from their Fig. 2) are needed to explain the cooling curve. Note that they include a prescription for boundary layer heating, while we have ignored this effect. The agreement between our results and Godon et al. (2004) indicates boundary layer heating is not important in the late time lightcurve (also see Appendix).

If we fit the last five out of eight temperatures measurements using the analytic formula from equation (20) instead of our numerical calculations, we find the best fit for $t_{\text{late}} = 39$ days with $T_{\text{eff},0} = 15,000 \text{ K}$. For this fit we assume a power law index of 0.81 because the current data does not allow us to treat it as a free parameter. This index value is fairly robust since both our work here and similar calculations using OPAL opacities give similar results. Using equation (22), this fit implies an accreted column $\Delta y = 1.1 \times 10^6 \text{ g cm}^{-2} g_8^{-2/21}$, within 20% of the full numerical lightcurve value. This shows the usefulness of our fitting formula for making quick estimates of the outburst properties. In general, equation (20) will over-predict $T_{\text{eff},0}$ because the lightcurve is merely approaches the power law asymptotically (as shown in Figure 6), so that its predicted columns are *lower limits*.

5. DISCUSSION AND CONCLUSIONS

We presented an investigation into the cooling of a WD after a DN outburst, focusing on late times when the luminosity from the WD is dominated by cooling of adiabatically compressed deep layers. We find that the lightcurve is a power law, *not* in $T_{\text{eff}}(t)$, but instead in $\delta T_{\text{eff}}(t)/T_{\text{eff},0}$. This results in a fitting function, equation (20), that can be used to constrain $T_{\text{eff},0}$ and the accreted column, Δy (eq. [22]), from the observations. The sensitivity to $T_{\text{eff},0}$ may be useful if outbursts are too closely spaced for the WD to ever cool to the quiescent temperature. Combining this with the work of Townsley & Bildsten (2003), would allow one to get a better handle on the long term accretion history over the CV’s lifetime. Previous studies that do this require careful measurements of $T_{\text{eff},0}$, but as our work shows, compressional heating during DN outbursts can have a long lasting impact on the flux leaving a WD. In our example models we find a 10% deviation from the quiescent flux 1000 days after the outburst has ended!

Our study highlights the importance of multiple measurements for a given outburst, over many epochs so as to tightly constrain the late time cooling. Many DN outbursts have only two measurements of their cooling lightcurve, so we cannot extend our analysis to these other systems. We made comparisons with WZ Sge because it is the best opportunity to test whether compressional heating is occurring and to see how well Δy and $T_{\text{eff},0}$ can be constrained, but even in this case the measurement errors are frustratingly large. It is encouraging that our work compares favorably to the outburst from this object, and we look forward to new, more detailed measurements that will test the effectiveness of our results. Multiple measurements would be a powerful tool in conjunction with our fitting function to study the properties of DN outbursts, especially in comparing multiple outbursts from the same system using equation (23).

The scalings and arguments we use may help to understand the heating of stellar surfaces in other environments.

APPENDIX

SURFACE HEATING

To this point we have neglected the effects of surface and shear heating. We now include the effect of a hot layer heating the WD surface, during the outburst and the subsequent cooling. Numerical runs with and without compressional heating are done for comparison, and we present analytical results for the case of surface heating alone. The result of our analysis is that a surface temperature $\gtrsim 10^6$ K is needed for an appreciable deviation from the analytic formula in equation (20). We conclude that surface heating has a negligible effect on late time cooling because the boundary layer is not sufficiently hot. These results also apply to heating due to the shearing of the surface accretion flow against the WD surface, because the shearing takes place at a column much less than those of interest for compressional heating (Piro & Bildsten 2004). Another mechanism that heats the surface is the advection of hot boundary layer fluid in the accretion flow as considered by Popham (1997). Such heating can only occur down to a column of Δy , and furthermore, this fluid quickly cools in the shallow surface layers near the boundary layer (because t_{th} is so short there), long before it can even reach this depth. Advection is therefore washed out by the surface heating at the depths of interest, which are many orders of magnitude deeper.

We follow Pringle (1988) and model boundary layer irradiation by enforcing a surface temperature T_{bl} during the outburst at the outermost grid point. However, surface heating from irradiation only occurs at low latitudes underneath the boundary layer. This has been shown both observationally (Mauche 2004) and theoretically (Piro & Bildsten 2004) to cover a small fraction of the WD surface area, $\epsilon_{\text{bl}} \sim 0.01 - 0.1$, while compressional heating occurs over the whole star. Hence, we assume that the lightcurve is generated by a fraction ϵ_{bl} of the star undergoing surface and compressional heating, and a fraction $1 - \epsilon_{\text{bl}}$ with compressional heating alone. In more detail, if $T_{\text{eff},1}$ includes only compressional heating and $T_{\text{eff},2}$ includes compressional and surface heating, we make a combined lightcurve as $T_{\text{eff}} = [(1 - \epsilon_{\text{bl}})T_{\text{eff},1}^4 + \epsilon_{\text{bl}}T_{\text{eff},2}^4]^{1/4}$. Other possible heating effects, such as irradiation through the radial flux in the disk (Regev 1983) or direct irradiation from the inner region of the accretion disk, will be of the same order as the ϵ_{bl} we consider here, and therefore do not need to be considered separately.

Figure A7 shows the temperature, temperature perturbation, and flux perturbation underneath the boundary layer at the end of the outburst, just before cooling begins. As T_{bl} is increased, the temperature profile is affected to larger depths. However, runs including both compressional and surface heating always show the $\delta T/T_0 \propto y^{-1}$ scaling at large depths, so we conclude: *surface heating can only propagate in a finite distance whereas compressional heating affects the material at arbitrarily large*

Such effects are observable whenever $t_{\text{th}}(\Delta y)$ is much longer than the characteristic viscous timescale in the outer accretion disk, and symbiotic binaries may be the most interesting case among such systems. Symbiotic binaries exhibit a variety of outburst types, one of which is commonly referred to as a “classical symbiotic outburst” (see Sokoloski 2004 for a recent review). In these outbursts the optical brightness increases by one to a few magnitudes over weeks or months and then decays over a timescale of months to years. The cause of classical symbiotic outbursts remains a mystery, but such timescales are characteristic of the DN outbursts we study here. The application of our work to these systems would test whether these outbursts are also accretion events. Symbiotics have a number of subtleties that must be correctly incorporated before they can be modeled, since they accrete at $\dot{M} \sim 10^{-9} - 10^{-6} M_{\odot} \text{ yr}^{-1}$, considerably higher rates than the DN systems. Consequently, there is a hotter boundary layer and a thicker disk, both of which increase the influence of surface heating (see Appendix). Another difference is that the temperature inversion we quickly mention in §2.2 is more pronounced when this much mass is accreted, but most likely it will still have a negligible effect on the late time cooling. The $T_{\text{eff},0}$ is higher for symbiotics because of a larger time-averaged accretion rate and possible steady nuclear burning (Sion & Starrfield 1994), and this helps to minimize any temperature inversion.

We thank Boris Gänsicke for providing comments on a previous draft of this paper and Danny Steeghs and Dean Townsley for thoughtful discussions. We also thank the anonymous referee for helpful comments and criticisms. This work was supported by the National Science Foundation under grants PHY99-07949 and AST02-05956, and by the Joint Institute for Nuclear Astrophysics through NSF grant PHY02-16783. Phil Arras is an NSF AAPF fellow.

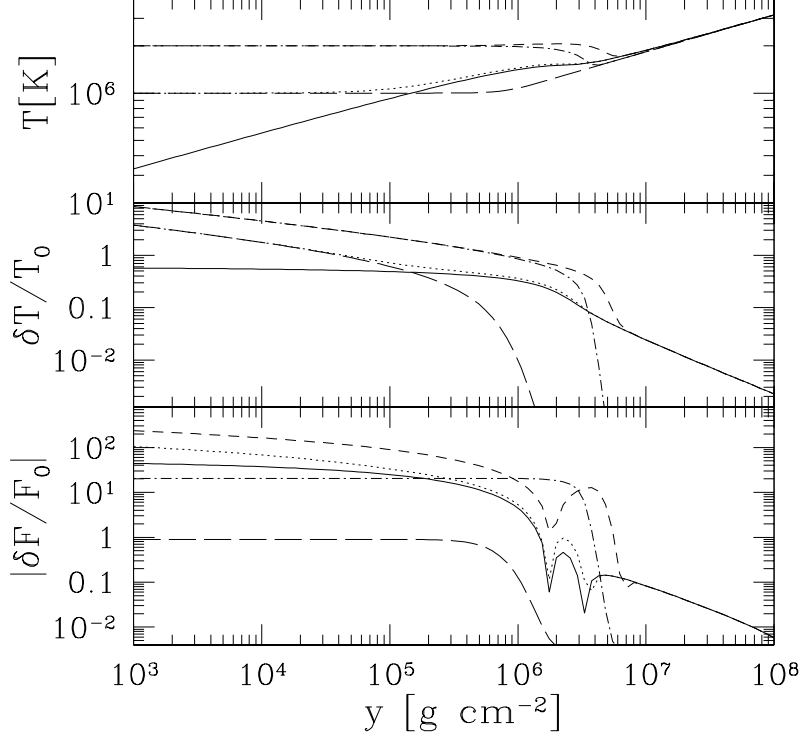


FIG. A7.— Temperature, fractional temperature perturbation, and fractional flux perturbation at the end of a 52 day outburst in which the star is heated by a boundary layer and/or compressional heating. The lines are $(\dot{m}[\text{g cm}^{-2} \text{ s}^{-1}], T_{\text{bl}}[\text{K}]) = (0.30, 0.0)$ (solid), $(0.30, 1.0 \times 10^6)$ (dotted), $(0.30, 2.0 \times 10^6)$ (short dash), $(0.0, 1.0 \times 10^6)$ (long dash), and $(0.0, 2.0 \times 10^6)$ (dot-dashed), all starting with a quiescent background model with $T_{\text{eff},0} = 14,500$ K.

depths. Hence, at late times the cooling must eventually be given by the analytic formulas in equations (20) and (22). In practice, for sufficiently high T_{bl} , this asymptotic scaling may occur so long after the outburst that for the entire observation period *both* heating mechanisms still affect the light curve. We will come back to this point.

Figure A8 shows cooling after the outburst. An accretion rate $\dot{m} = 0.30 \text{ g cm}^{-2} \text{ s}^{-1}$ was used for all curves, as in Figure A7. The curves with surface heating use 10% of the surface area being heated by the boundary layer, a plausible upper limit. The three curves represent compressional heating alone (solid line), and compressional and surface heating, weighted by the surface area, for $T_{\text{bl}} = 1.0 \times 10^6$ K (dotted line) and $T_{\text{bl}} = 2.0 \times 10^6$ K (dashed line), respectively. Surface heating is quite sensitive to T_{bl} , as the curve with $T_{\text{bl}} = 1.0 \times 10^6$ K is identical to that with no boundary layer heating, while the curve with $T_{\text{bl}} = 2.0 \times 10^6$ K shows 1% differences in T_{eff} at 1000 days.

For the fiducial accreted column used in this appendix, which is the column inferred for the July 2001 outburst of WZ Sge in §4, surface heating does *not* affect the lightcurve when the surface area is taken into account. As we have probably used an overestimate of the covering fraction ϵ_{bl} , one would have to increase T_{bl} to much larger values to compete with compressional heating at late times. Such high boundary layer temperatures are inconsistent with models calculated by Piro & Bildsten (2004) for $\dot{M} \approx 2 \times 10^{-8} M_{\odot} \text{ yr}^{-1}$, which is still more than the average accretion rate we infer in §4 for during the outburst of WZ Sge of $10^{-8} M_{\odot} \text{ yr}^{-1}$.

We now explain the qualitative features seen in Figures A7 and A8. The hot boundary initiates a thermal wave propagating into the star. The column depth to which this nonlinear diffusion wave propagates is estimated from equations (1) and (4)

$$\begin{aligned}
 y_{\text{diff}}(t) &\sim \left(\frac{\alpha t}{c_p} T_{\text{bl}}^{3+a-b} \right)^{1/(a+2)} \\
 &\approx 1.1 \times 10^7 \text{ g cm}^{-2} g_8^{-1/3} \left(\frac{T_{\text{bl}}}{10^6 \text{ K}} \right)^{17/6} \left(\frac{t}{1 \text{ day}} \right)^{1/3}, \quad (\text{A1})
 \end{aligned}$$

where $T_{\text{bl},6} \equiv T_{\text{bl}}/10^6 \text{ K}$. At depths smaller than $y_{\text{diff}}(t)$, the temperature is nearly T_{bl} and the flux is approximately constant with the value

$$\begin{aligned}
 F &\sim \alpha \frac{T_{\text{bl}}^{4+a-b}}{y_{\text{diff}}^{a+1}(t)} \\
 &\approx 10^{14} \text{ erg cm}^{-2} \text{ s}^{-1} g_8^{-1/3} \left(\frac{T_{\text{bl}}}{10^6 \text{ K}} \right)^{7/2} \left(\frac{t}{1 \text{ day}} \right)^{-2/3}. \quad (\text{A2})
 \end{aligned}$$

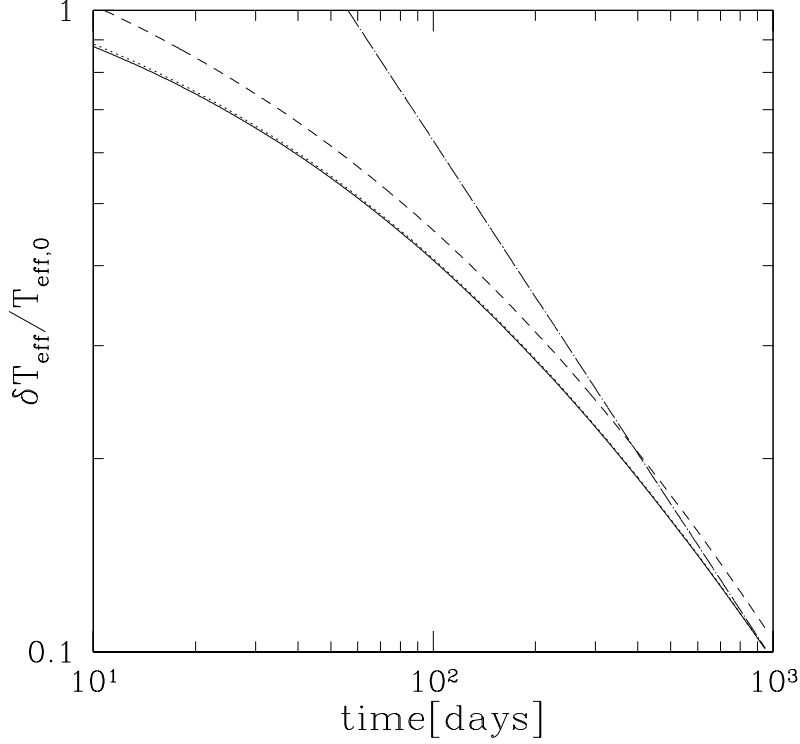


FIG. A8.— T_{eff} perturbation as a function of time after end of the outburst of duration 52 days. Lightcurves were generated for $(\dot{m}[\text{g cm}^{-2} \text{ s}^{-1}], T_{\text{bl}}[\text{K}]) = (0.30, 0.0)$, $(0.30, 1.0 \times 10^6)$, $(0.30, 2.0 \times 10^6)$. These lightcurves were then weighted by the fraction (10%) of surface area undergoing heating, as described in the text. The curves represent compressional heating alone (solid line), compressional and surface heating for $T_{\text{bl}} = 1.0 \times 10^6$ K (dotted line) and $T_{\text{bl}} = 2.0 \times 10^6$ K (dashed line), all for a quiescent background model with $T_{\text{eff},0} = 14,500$ K. The dot long-dashed line is the analytic formula from equations (20) and (22).

Given a sufficient outburst duration, $t_{\text{dno}} \gtrsim 3 \text{ yr } g_8^{-1/2} F_{0,12}^{-3/2} (T_{\text{bl}}/10^6 \text{ K})^{21/4}$, the thermal wave will penetrate to a depth at which T_{bl} is equal to the background temperature profile. This occurs at a column

$$y_{\text{bl}} = \left[(n+1) \frac{F_0}{\alpha} \right]^{-1/(a+1)} T_{\text{bl}}^{n+1} \approx 1.2 \times 10^6 \text{ g cm}^{-2} g_8^{-1/2} F_{0,12}^{-1/2} \left(\frac{T_{\text{bl}}}{10^6 \text{ K}} \right)^{17/4}. \quad (\text{A3})$$

A simple estimate for when surface heating will affect the late time cooling is to set y_{bl} equal to the accreted column Δy . At this point, the temperature perturbation due to compressional heating becomes small ($\delta T/T_0 \ll 1$), and additional boundary layer heating can delay the late time power law. We find the critical boundary layer temperature

$$T_{\text{bl,crit}} \sim 10^6 \text{ K } g_8^{2/17} F_{0,12}^{2/17} \left(\frac{\Delta y}{10^6 \text{ g cm}^{-2}} \right)^{4/17}, \quad (\text{A4})$$

consistent with Figure A7. This derivation only considers layers directly below where surface heating is occurring, so that if $\epsilon_{\text{bl}} \ll 1$ then $T_{\text{bl,crit}}$ must be somewhat larger. Nevertheless, this still provides a useful lower limit for when the boundary layer may be important. It is interesting that this $T_{\text{bl,crit}}$ is comparable to, but most likely ruled out by, observations (Mauche 2004) and theoretical modeling (Popham & Narayan 1995; Piro & Bildsten 2004) of boundary layer temperatures. If T_{bl} is larger than this critical value, the cooling profile does not reach our analytic result in an observable amount of time, as shown in Figure A8, so that if our fitting formula is incorrectly applied it will result in an overprediction of Δy .

Now consider surface heating at large depths, ignoring compressional heating for simplicity. At depths $y \gg y_{\text{bl}}$, the temperature perturbations become small, and linear theory is again applicable. Using the same method as in §3, we insert the ansatz $\delta T/T_0 = f(\xi)$ into equations (1) and (4), where $\xi = [t_{\text{th},0}(y)/t]^{1/2}$ uses the thermal time of the background state. We can derive a self-similar equation for the temperature perturbation at large depths during heating, which we do not present here. As we desire the temperature perturbations deep in the envelope, we take the $\xi \gg 1$ limit, finding the simpler equation

$$\frac{d^2 f}{d\xi^2} \approx -\frac{2(n+1)}{(n+2)^2} \xi \frac{df}{d\xi}, \quad (\text{A5})$$

with a solution at $t = t_{\text{dno}}$ of

$$\begin{aligned} \frac{\delta T}{T_0} &\approx f \propto \xi^{-1} \exp(-\lambda \xi^2) \\ &\sim \left[\frac{t_{\text{dno}}}{t_{\text{th},0}(y)} \right]^{1/2} \exp \left[-\lambda \frac{t_{\text{th},0}(y)}{t_{\text{dno}}} \right], \end{aligned} \quad (\text{A6})$$

where $\lambda = (n+1)/(n+2)^2 \approx 0.154$. Hence the temperature perturbations “tunneling” further than y_{bl} are exponentially small, as seen in the rapid dropoffs in Figure A7. The small factor $\lambda \ll 1$ implies that the dropoff occurs at a column an order of magnitude larger than one would naïvely expect.

REFERENCES

- Bildsten, L. 1998, in *The Many Faces of Neutron Stars*, ed. R. Buccheri, J. van Paradijs, & A. Alpar (Dordrecht: Kluwer), 419
- Cheng, F. H., Horne, K., Marsh, T. R., Hubeny, I., & Sion, E. M. 2000, *ApJ*, 542, 1064
- Gänsicke, B. T. & Beuermann, K. 1996, *A&A*, 309, L47
- Godon, P., Regev, O., & Shaviv, G. 1995, *MNRAS*, 275, 1093
- Godon, P. & Sion, E. M. 2002, *ApJ*, 566, 1084
- Godon, P. & Sion, E. M. 2003, *ApJ*, 586, 427
- Godon, P., Sion, E. M., Cheng, F., Gänsicke, B. T., Howell, S., Knigge, C., Sparks, W. M., & Starrfield, S. 2004, *ApJ*, 602, 336
- Iglesias, C. A. & Rogers, F. J. 1996, *ApJ*, 464, 943
- Ishioaka, R., et al. 2001, *IAU Circ.*, 7669, 1
- Kiplinger, A., Sion, E. M., & Szkody, P. 1991, *ApJ*, 366, 569
- Long, K. S., Froning, C. S., Gänsicke, B. T., Knigge, C., Sion, E. M., & Szkody, P. 2003, *ApJ*, 591, 1172
- Long, K. S., Blair, W. P., Bowers, C. W., Davidson, A. F., Kriss, G. A., Sion, E. M., & Hubeny, I. 1993, *ApJ*, 405, 327
- Long, K. S., Sion, E. M., Huang, M., & Szkody, P. 1994, *ApJ*, 424, L49
- Long, K. S., Sion, E. M., Gänsicke, B. T., & Szkody, P. 2004, *ApJ*, 602, 948
- Mateo, M. & Szkody, P. 1984, *AJ*, 89, 863
- Mauche, C. W. 2004, *ApJ*, 610, 422
- Patterson, J. et al. 2002, *PASP*, 114, 721
- Piro, A. L. & Bildsten, L. 2004, *ApJ*, 610, 977
- Popham, R. 1997, *ApJ*, 478, 734
- Popham, R. & Narayan, R. 1995, *ApJ*, 442, 337
- Pringle, J. E. 1988, *MNRAS*, 230, 587
- Regev, O. 1983, *A&A*, 126, 146
- Regev, O. & Shara, M. M. 1989, *ApJ*, 340, 1006
- Sion, E. M. 1993, *Ann. Israel Phys. Soc.*, 10, 86
- Sion, E. M. 1995, *ApJ*, 438, 876
- Sion, E. M., Cheng, F. H., Huang, M., Hubeny, I., & Szkody, P. 1996, *ApJ*, 471, L41
- Sion E. M. & Starrfield S. G., 1994, *ApJ*, 421, 261
- Szkody, P., Hoard, D. W., Sion, E. M., Howell, S. B., Cheng, F. H., & Sparks, W. M. 1998, *ApJ*, 497, 928
- Sokoloski, J. L. 2004, to appear in the *Journal of the American Association of Variable Star Observers (AAVSO)*, astro-ph/0403004
- Sparks, W. M., Sion, E. M., Starrfield, S. G., & Austin, S. 1993, *Ann. Israel Phys. Soc.*, 10, 96
- Townsley, D. M. & Bildsten, L. 2003, *ApJ*, 596, L227
- Warner, B. 1995, *Cataclysmic Variable Stars* (Cambridge: Cambridge Univ. Press)